Testing the Validity of the Miscible-Displacement Interfacial Tracer Method for Measuring Air-Water Interfacial Area: Independent Benchmarking and Mathematical Modeling

Asma El Ouni¹, Bo Guo², Hua Zhong³, and Mark L. Brusseau^{1,2,*}

¹Environmental Science Department

²Hydrology and Atmospheric Sciences Department

University of Arizona

Tucson, AZ 85721

³State Key Laboratory of Water Resources and Hydropower Engineering Science, Wuhan

University, Wuhan, Hubei, 430072, PR China

Submitted to:

Chemosphere

June 18, 2020

Revised: August 24, 2020

*Corresponding author, Brusseau@email.arizona.edu

1 ABSTRACT

The interfacial tracer test (ITT) conducted via aqueous miscible-displacement column
experiments is one of a few methods available to measure air-water interfacial areas for porous
media. The primary objective of this study was to examine the robustness of air-water interfacial
area measurements obtained with interfacial tracer tests, and to examine the overall validity of the
method. The potential occurrence and impact of surfactant-induced flow was investigated, as was
measurement replication. The column and the effluent samples were weighed during the tests to
monitor for potential changes in water saturation and flux. Minimal changes in water saturation
and flux were observed for experiments wherein steady flow conditions were maintained using a
vacuum-chamber system. The air-water interfacial areas measured with the miscible-displacement
method completely matched interfacial areas measured with methods that are not influenced by
surfactant-induced flow. This successful benchmarking was observed for all three media tested,
and over a range of saturations. A mathematical model explicitly accounting for nonlinear and
rate-limited adsorption of surfactant at the solid-water and air-water interfaces as well as the
influence of changes in surface tension on matric potentials and flow was used to simulate the
tracer tests. The independently-predicted simulations provided excellent matches to the measured
data, and revealed that the use of the vacuum system minimized the occurrence of surfactant-
induced flow and its associated effects. These results in total unequivocally demonstrate that the
miscible-displacement ITT method produced accurate and robust measurements of air-water
interfacial area under the extant conditions.

Keywords: air-water interface; tracer test; adsorption; unsaturated; surfactant-induced flow.

1. Introduction

It is widely recognized that the air-water interface plays a fundamental role in the distribution and flow of water and other fluids in unsaturated porous media. Mass and energy transfer processes such as evaporation, volatilization, gas exchange, and heat flow occur at this interface. In addition, the air-water interface can have a major impact on the retention and transport of materials, including colloids and organic contaminants. The vadose zone mediates the transmission of contaminants from the land surface to groundwater. Thus, understanding contaminant transport in this multi-phase system is critical for accurate characterization of groundwater contamination potential.

While the importance of the air-water interface in porous media has long been established, it has taken on enhanced significance with the issue of per- and poly-fluoroalkyl substances (PFAS) in the environment. PFAS are a class of synthetic fluorinated surfactants that have been and are used in a wide variety of consumer products and industrial materials. Research has demonstrated that they are widespread in the environment and pose potential risks to human health. Of particular note, soil has been delineated as a major reservoir of PFAS (Anderson et al., 2019; Brusseau et al., 2020a; Guo et al., 2020), and a critical concern is the leaching behavior of PFAS and their potential to contaminate groundwater. Adsorption at the air-water interface is a primary retention process for PFAS transport in unsaturated media (Brusseau, 2018; Lyu et al., 2018; Brusseau et al., 2019; Lyu and Brusseau, 2020). Air-water interfacial adsorption has also been identified to be important for the retention and transport of other emerging contaminants, including antibiotics (Dong et al., 2016) and nanoparticles (Kumahor et al., 2015; Makselon et al., 2017).

Characterizing and modeling multiphase fluid flow, interfacial mass-transfer processes, and the transport of interfacial-active substances requires accurate determination of air-water interfacial areas. Interfacial tracer tests (ITT) are one of the few methods available to measure air-

water interfacial area in porous media (e.g., Karkare and Fort, 1996; Brusseau et al., 1997; Kim et al., 1997; Saripalli et al., 1997; Kim et al., 1999; Anwar et al., 2000; Anwar, 2001; Schaefer et al., 2000; Costanza-Robinson and Brusseau, 2002; Peng and Brusseau, 2005; Araujo et al., 2015). ITT tests can be implemented in several ways. One standard approach is to conduct aqueous miscible-displacement tracer tests wherein an aqueous solution containing a tracer that preferentially adsorbs at the air-water interface is injected into a packed column under steady unsaturated-flow conditions. This method was introduced by Rao and colleagues (Kim et al., 1997; Saripalli et al., 1997), and has since been used in multiple additional studies (e.g., Kim et al., 1998; Brusseau et al., 2007; Costanza-Robinson et al., 2012; Brusseau et al., 2015, 2020b).

A surfactant or other interfacial-active solute is used as the interfacial tracer for ITTs. One potential concern associated specifically with the miscible-displacement-based ITT method is the occurrence of surfactant-induced flow due to the change in surface tension upon the introduction and displacement of the surfactant solution (Kim et al., 1997). Surfactant-induced flow can add uncertainty to the determination of interfacial areas and should be assessed when employing this method. Brusseau et al. (2007) conducted miscible-displacement IT tests and showed no impact of surfactant-induced flow when employing a vacuum system. Conversely, Costanza-Robinson et al. (2012) observed surfactant-induced flow for miscible-displacement IT tests conducted with a hanging water-column system. Costanza-Robinson and Henry (2017) conducted mathematical modeling simulations of IT tests for hypothetical systems and concluded that surfactant-induced flow invariably affects all miscible-displacement IT tests and, therefore, that interfacial areas so obtained have significant uncertainty.

The issue of the robustness of air-water interfacial areas measured with the miscibledisplacement IT test is critical to resolve as this method is one of the few available that can be readily employed in a standard laboratory setting and without the need for advanced specialized instrumentation. The dearth of independent measurements of air-water interfacial area has limited the ability of prior studies to investigate the accuracy and robustness of interfacial areas measured with the miscible-displacement IT method. Such data are now available and can be used as independent benchmarks for comparative assessments. Another effective means of assessing robustness is the use of mathematical modeling, with the specific approach of employing a distributed-process model in forward-solution mode such that independent predictions of transport are produced. Such mathematical modeling has not been applied to actual miscible-displacement ITT data in prior studies. Another issue of import for method robustness is that of measurement uncertainty. Prior miscible-displacement IT studies have not examined measurement uncertainty by conducting multiple replicate measurements.

The objective of the present study is to examine the accuracy and robustness of air-water interfacial area measurements obtained with the aqueous miscible-displacement ITT method. The potential occurrence and impact of surfactant-induced flow will be investigated, as will measurement replication. Independent benchmarking analysis is conducted by comparing the interfacial areas measured with the miscible-displacement ITT method to measurements obtained with alternative methods that are not influenced by surfactant-induced flow. Mathematical modeling is employed to characterize flow and transport behavior associated with the miscible-displacement system, and to directly examine the impact of surfactant-induced flow. The modelling is novel in that it is used specifically to produce independent-prediction simulations of the measured breakthrough curves and solution flux, which represents to our knowledge the first attempt to do so for the miscible-displacement ITT method.

2. Materials and Methods

2.1. Materials

Three porous media were used in this study. Vinton soil (sandy, mixed thermic Typic Torrifluvent), collected locally in Tucson, AZ., a 45/50 mesh quartz sand (Accusand), and borosilicate glass beads with a relatively large diameter (1.16 mm). Vinton soil was sieved to remove the fraction larger than 2 mm. Relevant properties of the porous media are presented in Table 1.

Sodium dodecyl benzene sulfonate (SDBS) was used as the air-water interfacial adsorptive tracer, with input concentrations of approximately 40 mg/L. Pentafluorobenzoic Acid (PFBA, 100 mg/L) was used as the nonreactive tracer to characterize the hydrodynamic properties of the packed columns. Sodium chloride (0.01 M) was used as the background electrolyte to maintain a constant ionic strength, thus minimizing potential changes in electrostatic properties.

The columns used for the tracer tests were constructed of stainless steel and were 15 cm long by 2.2 cm in diameter. Each column was packed with air-dried media to obtain uniform bulk densities. The columns were oriented vertically for all experiments. A stainless steel distribution plate and a porous frit were placed at the bottom of the column to retain the solids and to maintain saturated conditions to promote uniform water flow. A distribution plate and a porous frit were placed at the top of the column for the saturated-flow experiments. The plate, frit, and endcap were removed from the top for the unsaturated-flow experiments.

A piston pump was used to provide a constant solution flow to the open top of the column for the unsaturated-flow experiments. Tubing from the bottom of the column was connected to a vacuum chamber that housed a fraction collector to which the column effluent line was connected for sample collection. This system allowed for effluent sample collection while a steady,

uninterrupted vacuum was maintained during the entire experiment. For four experiments (2 Vinton and 2 sand), a flask apparatus instead of the vacuum chamber was used for the sample collection. In this case, the vacuum is interrupted when valves are switched during sample collection.

2.2. Methods

The surface tension of the SDBS-electrolyte solution was measured using a Du Nouy ring tensionmeter (Fisher Scientific, Surface Tensiomat 21) following standard methods. The tensiometer was calibrated with a weight of known mass. Each sample was measured at least three times with a deviation between measurements of less than 1%. Two separate sets of measurements were conducted by different students several years apart. In addition, data for the same SDBS-electrolyte system was collected from the literature for comparison.

The methods used for the miscible-displacement experiments were the same as used by Brusseau et al. (2007), who reported air-water interfacial areas for the Vinton soil. One set of experiments was conducted in the present study to examine measurement replication uncertainty. Thus, five additional tests were conducted for the Vinton soil at the same water saturation (~0.8) to supplement two prior measurements reported in the Brusseau et al. (2007) study. A second set of two experiments was conducted for Vinton at a lower water saturation to combine with the eight experiments reported in Brusseau et al. (2007). A third set of experiments was conducted in the present study to measure air-water interfacial areas for the sand (6 experiments) and glass beads (2 experiments), which were not used in the prior 2007 study. Two nominal flow rates were used for the Brusseau et al. (2007) study, 0.5 and 0.2 mL/min, equivalent to mean pore-water velocities of approximately 18 and 9 cm/h, respectively. A flow rate of 0.5 mL/min was used for all

experiments for the present study, with one exception of 0.2 for a replicate Vinton test at a water saturation of 0.77.

Experiments for Vinton soil were conducted under both primary drainage and primary imbibition conditions, whereas the experiments for the sand and glass beads were conducted under primary drainage. For imbibition conditions, electrolyte solution was introduced to the top of the dry packed column while it was connected to the vacuum system. For drainage conditions, the packed column was completely saturated with electrolyte solution prior to initiation of drainage. The initial saturation step was conducted using a separate apparatus wherein electrolyte solution was injected into the bottom of the column. The mass of the column was measured periodically, and complete saturation was assumed once the measurement stabilized. Note that a hanging water-column method was used for the glass beads, as the vacuum system reduced water saturation to levels too low to maintain adequate flow.

The tracer tests were conducted after steady-state flow was established at the desired water saturation. Each set of tracer tests was performed in a newly prepared column, and the nonreactive and adsorptive tracer tests were conducted sequentially. Each effluent sample was weighed (measurement uncertainty = \sim 0.002%) and the mass of the solution reservoir was monitored (measurement uncertainty = <0.1%), providing a means of monitoring for potential variations in the amount of solution exiting the column and determination of any changes in water saturation of the packed column. The mass of the column was also measured periodically as a second determination of changes in water saturation (measurement uncertainty = <1%). Tracer tests were conducted under water-saturated conditions to measure the adsorption of SDBS by the solid matrix. Effluent samples were analyzed by UV-Vis spectrophotometry. Additional details of the method are reported in Brusseau et al. (2007).

2.3. Data Analysis

The ITT method consists of conducting miscible-displacement tracer tests, from which retardation factors, R, are determined from the breakthrough curves using standard frontal and moment analyses (e.g., Kim et al., 1997; Brusseau et al., 2007). Numerous theoretical and experimental works have demonstrated that these methods produce accurate measures of R and associated distribution coefficients independent of nonideal adsorption constraints (Glueckauf, 1955; Kucera, 1965; Buffham, 1973; Valocchi, 1985). Kim et al. (1997) discuss this specifically for application to the analysis of miscible-displacement ITT data. Costanza-Robinson and Henry (2017) demonstrated with mathematical modeling that this analysis approach recovered representative R and air-water interfacial area values for simulated miscible-displacement IT tests.

The measured R-values are used in conjunction with equation 1 to determine interfacial area (with all other variables known):

$$R = 1 + K_d \frac{\rho_b}{\theta_w} + K_i \frac{A_{ia}}{\theta_w} \tag{1}$$

where K_d (cm³/g) is the sorption coefficient to the solid, ρ_b (g/cm³) is the bulk density, θ_w is the volumetric water content, K_i (cm) is the interfacial adsorption coefficient, and A_{ia} (cm⁻¹) is the specific air-water interfacial area (interfacial area normalized by the porous-medium volume, cm²/cm³). The K_d is determined by conducting the tracer tests under water-saturated conditions. The K_i is determined from the measured surface-tension function for the selected input concentration (e.g., Kim et al., 1997; Brusseau et al., 2007). It is important to note that the ITT method provides a measure of the "total" air-water interfacial area, and includes contributions of capillary (meniscus) and film-associated areas. Note that the interfacial areas for the data reported in Brusseau et al. (2007) were recalculated using the updated K_i value obtained from the aggregated surface-tension data. This maintains consistency among the prior and new data sets.

2.4. Mathematical Modeling

A one-dimensional numerical model that couples transient, variably saturated flow and solute transport (Guo et al., 2020) was used to investigate the potential for surfactant-induced flow under the extant experiment conditions. The model simulates the impact of an interfacial tracer on surface tension, and the subsequent influence on displacement of the solution. The model also simulates transport of the interfacial tracer, and explicitly accounts for nonlinear and rate-limited adsorption at the solid-water and air-water interfaces. The baseline equations for flow and transport are presented in Guo et al. (2020). The following paragraph details the modification made to account for specific conditions of the tracer tests.

When a vacuum pump is applied at the outlet, the Richards equation for variably saturated flow needs to be modified to account for the vacuum pressure in the air phase. Denoting the water pressure head as h_w , water flux in the column may be described by the two-phase extended Darcy's Law as

$$q = -K \left(\frac{\partial h_w}{\partial z} - 1 \right), \tag{2}$$

where K (cm/min) is unsaturated hydraulic conductivity and z (cm) is the vertical axis along the column (assuming positive downward). The water pressure head is related to the air pressure (h_a , with a unit of cm w.r.t. water) and capillary pressure (h_c , with a unit of cm w.r.t. water) heads as $h_w = h_a - h_c$. Substituting $h_w = h_a - h_c$ to Eq. (2) yields

$$q = -K\left(-\frac{\partial h_c}{\partial z} + \frac{\partial h_a}{\partial z} - 1\right). \tag{3}$$

The air pressure head at the inlet is zero (open to the atmosphere). The air pressure head at the outlet is negative due to the vacuum pump, i.e., $h_a = h_{a,0}$, where $h_{a,0}$ is the vacuum pressure head. Assuming that air flow is approximately steady-state and maintains a linear pressure distribution

along the column during the experiment, we obtain $\frac{\partial h_a}{\partial z} \approx \frac{h_{a,0}-0}{L}$, where L (cm) is the length of the column. Therefore, Eq. (3) can be rewritten as

$$q = -K \left[-\frac{\partial h_c}{\partial z} + \frac{h_{a,0}}{L} - 1 \right]. \tag{4}$$

Substituting Eq. (4) into the mass balance equation for water yields a modified Richards equation as follows

$$\frac{\partial \theta_{w}}{\partial t} - \frac{\partial}{\partial z} \left[K \left(-\frac{\partial h_{c}}{\partial z} + \frac{h_{a,0}}{L} - 1 \right) \right] = 0.$$
 (5)

We replace the Richards equation in the model of Guo et al. (2020) with Eq. (5) to simulate the column experiments that employ a vacuum pump at the outlet. Everything else remains the same. Note that Eq. (5) recovers the standard Richards equation with $h_{a,0} = 0$ when no vacuum is applied at the outlet. The coupled equations of flow and transport are solved by a fully implicit numerical framework using Newton-Raphson iterations. Details of the equations and numerical methods are provided in Guo et al. (2020).

Illustrative simulations are presented for the miscible-displacement tracer tests conducted with the sand. Two sets of simulations are conducted, one with the vacuum applied and one without. The simulation domain is vertical with a length of 14.7 cm and is discretized into 294 numerical cells with a uniform size. The upper boundary is set as constant flux with an infiltration rate of 0.13 cm/min. The lower boundary is set as free drainage. Initially, the domain is under steady-state flow at 0.13 cm/min. The interfacial tracer solution with a concentration of 40.9 mg/L is applied at time zero and stopped at t = 4 hours. The simulation lasts for 8 hours. The vacuum pressure at the outlet is $h_{a,0} = -100$ cm. All parameters used for the simulations were obtained from independent measurements, including saturated hydraulic conductivity $K_{sat} = 0.048$ cm/min, porosity n = 0.326, residual water content $\theta_r = 0.015$, diffusion coefficient $D_m = 4.9 \times 10^{-10}$

 10^{-6} cm²/s, longitudinal dispersivity $\alpha_L = 0.29$ cm, Freundlich solid-phase adsorption coefficients $K_f = 0.107 \, / \mathrm{kg/(mg/L)^n}$ and n = 0.85, bulk density $\rho_b = 1.66 \, \mathrm{g/cm^3}$. A twodomain nonlinear, rate-limited adsorption model is used for both solid-phase and air-water interfacial adsorption. The fraction of sorbent for which solid-phase sorption is instantaneous F_s 0.37, the first-order rate constant for rate-limited solid-phase adsorption $\alpha_s = 2.6$ hour⁻¹. The adsorption at all air-water interfaces is assumed rate-limited ($F_{aw} = 0$) with a first-order rate constant of $\alpha_{aw} = 7$ hour⁻¹. Values for the adsorption parameters were obtained from Brusseau (2020). Note that a greater saturated conductivity was used for the no vacuum-pump simulation to maintain the same flow rate. The measured soil water characteristic curve and unsaturated hydraulic conductivity are modeled with the van Genuchten-Mualem model (Mualem, 1976; van Genuchten, 1980) with the parameters $\alpha = 0.0448 \text{ cm}^{-1}$ and n = 4. The air-water interfacial area is represented as an empirical function of water saturation based on aggregated measurements reported in Jiang et al. (2020). The fitting coefficients for the empirical function for sand are provided in Guo et al. (2020). The surface tension γ and K_i are determined using the measured surface-tension data for SDBS.

245

246

247

248

249

250

251

252

230

231

232

233

234

235

236

237

238

239

240

241

242

243

244

3. Results and Discussion

3.1 Surface Tension

Measured surface tensions for SDBS in 0.01 M NaCl solution are presented in Figure 1. Two sets of measurements were conducted several years apart for the present study (UAZ-1 and UAZ-2). In addition, published data for SDBS for the same 0.01 M NaCl solution reported in two prior studies are included for comparison. There is very good correspondence among all four sets of measurements. This provides confidence in the accuracy of the measurements and in the K_i

value determined from the data. The Szyszkowski equation provides a good fit to these combined four data sets. A K_i value of 2.6 x 10^{-3} cm is determined for the relevant concentration used for the tests.

3.2 Tracer Transport and Water Saturation

The breakthrough curves for PFBA, the nonreactive tracer, exhibit ideal transport behavior for all experiments under both water-saturated and unsaturated conditions (see Figure 2). The breakthrough curves for SDBS under saturated-flow conditions exhibit a small degree of tailing due to a combination of rate-limited and nonlinear adsorption (see Figure 2A for an example). The breakthrough curves for SDBS transport under unsaturated-flow conditions also exhibit tailing (Figure 2).

The mean retardation factors for SDBS under water-saturated conditions are approximately 3 for the Vinton soil, 1.3 for the sand, and 1.1 for the glass beads. This retardation is due to surfactant sorption to the solid media. The retardation of SDBS under unsaturated conditions is larger than under saturated conditions due to SDBS retention at the air-water interface (see Figure 2A for an example). The results of replicate tests displayed good reproducibility, as illustrated in Figure 2B.

A total of 13 sets of tracer tests were conducted under unsaturated conditions for the Vinton soil and the sand in this study. Mean changes in water saturation of ~1% or less were measured for the Vinton and sand tests for which the vacuum-chamber system was used. These values are within measurement uncertainty, demonstrating that no statistically significant drainage was observed for these tests. Conversely, a moderate degree of drainage was observed for the tests for which the vacuum chamber was not used, with a mean change in saturation of ~15%. The disparity

in observed results suggests that the interruption of the vacuum influenced the occurrence and/or magnitude of surfactant-induced flow.

3.3 Air-water Interfacial Areas

The air-water interfacial areas measured for the three media are presented in Figures 3-5. The interfacial areas for the glass beads are approximately 20 cm⁻¹ for water saturations of ~0.3 (Figure 3). The accuracy of these values can be evaluated by comparing them to air-water interfacial areas measured by synchrotron x-ray microtomography (XMT). The XMT method has been demonstrated via independent benchmarking analysis to produce robust measures of air-water interfacial area for coarse-grained monodisperse media (Araujo and Brusseau, 2020).

Inspection of Figure 3 shows that the interfacial areas measured by the ITT method are fully coincident with the XMT measurements. This observation is consistent with results reported by Narter and Brusseau (2010), who demonstrated consistency between ITT and XMT measurements of NAPL-water interfacial areas for the same glass-bead medium. These consistent results for the air-water IT tests were obtained with the use of a hanging water column for the experiments, albeit at a relatively low water saturation.

It is notable that the geometric smooth-surface solid surface area is essentially identical to the solid surface area measured with the nitrogen-BET method for these glass beads (see Table 1). In addition, the solid surface area measured by direct imaging of the solids with XMT is also the same as the geometric and NBET surface areas (Araujo and Brusseau, 2020). This congruence of solid surface area measurements is a manifestation of the fact that the glass beads have no measurable surface roughness. For an ideal medium such as these glass beads, XMT measures all air-water interfaces present in the system (Araujo and Brusseau, 2020). Critically, the

measurements are not affected by tracer-accessibility constraints, surfactant-induced flow issues, or other factors that can impact the ITT method. The fact that the ITT-measured interfacial areas match those measured by XMT indicates that the interfacial areas measured by the ITT method are accurate.

Air-water interfacial areas measured for the sand across a relatively large range of water saturation are presented in Figure 4. The values are observed to increase with decreasing saturation, as expected, ranging from ~30 to ~130 cm⁻¹. The values are compared to air-water interfacial areas measured for the same sand in a prior study conducted with the ITT method, but employing surfactant concentrations of 1, 0.1, and 0.01 mg/L (Brusseau et al., 2020b). Data analysis and mathematical modeling demonstrated conclusively that surfactant-induced flow did not occur for these low-concentration tracer tests.

Both sets of measurements are observed to be coincident along the same curve (Figure 4). Thus, interfacial areas measured with the standard ITT method employing tracer concentrations of ~40 mg/L are fully consistent with those measured using much lower concentrations for which surfactant-induced flow is irrelevant. This indicates that the measurements made using the higher concentrations are robust, and are not influenced measurably by surfactant-induced flow.

Air-water interfacial areas measured for the Vinton soil are presented in Figure 5. The values are observed to increase nonlinearly with decreasing water saturation, increasing from ~50 to 300 cm⁻¹. The results incorporate tests conducted at two different flow rates, one approximately two-times greater than the other. The results for the two sets of measurements are consistent, indicting no measurable impact of residence time over this range.

An analysis of measurement replication uncertainty for Vinton is presented in Table 2, wherein the mean, 95% confidence interval, and coefficient of variation (COV) are reported for

seven replicate measurements at a water saturation of \sim 0.81. The mean value is 66.2, with a confidence interval of 6 cm⁻¹. The COV is 9%, which is quite low especially considering that each test was conducted with a new column pack and by different personnel several years apart. It is also notable that the COV for water saturation is extremely low, showing that the use of the vacuum system promotes robust replication of target water saturations.

The mean air-water interfacial area measured with the standard ITT method at the 0.81 water saturation is compared in Table 2 to values measured with two alternative ITT methods developed by Brusseau et al. (2015). The first alternative method, named the dual-surfactant method, employs a second surfactant in the background electrolyte solution. The use of the two surfactants, one for the background solution and the other to serve as the interfacial tracer, prevents the formation of surface-tension gradients and thus eliminates surfactant-induced flow. The second alternative method, named the residual-air method, is based on establishing a discontinuous (residual) saturation of air prior to the test. This promotes single-phase flow conditions with no surfactant-induced flow.

The interfacial areas measured with the two alternative methods are both ~61cm⁻¹ at the same 0.81 water saturation. These values are within the 95% CI determined for the measurements made with the standard miscible-displacement ITT method (Table 2). This consistency among the three methods indicates that the interfacial areas measured with the standard ITT method are robust, and not influenced measurably by surfactant-induced flow.

One of the seven experiments listed in Table 2 was conducted without the vacuum chamber, whereas the other six were. While no measurable change in water saturation was observed for the latter six, the mean water saturation decreased temporarily by a maximum of 7.5% for the experiment conducted without the chamber. In this case, the interfacial area was calculated

using the mean water saturation. Inspection of Table 2 shows that the air-water interfacial area determined for this experiment is consistent with the other six values. Similarly, two experiments for the sand were conducted without the vacuum chamber and exhibited changes in water saturation. However, the air-water interfacial areas determined for these two experiments using mean saturations (the two lowest water-saturation data points in Figure 4) are consistent with all other values. This indicates that consistent air-water interfacial areas were obtained for the few experiments for which moderate changes in water saturation were observed (i.e., those conducted without the chamber).

Four of the seven tests presented in Table 2 were conducted under primary drainage while three were conducted under primary imbibition. Inspection of Table 2 shows that the two sets of values are consistent. In addition, there is no statistical difference in the means of the two sets of values (67 vs 65), and furthermore the two means are very similar to the aggregate mean. These results suggest that there is no measurable impact of initial fluid disposition on measured interfacial areas. This is likely a reflection of film-associated interfaces contributing the majority of total area (Or and Tuller, 1999; Brusseau et al., 2007; Jiang et al., 2020).

The measured air-water interfacial areas are largest for the soil, smallest for the glass beads, and intermediate for the sand for a given water saturation. The disparity in interfacial areas between the three porous media can be attributed to the differences in median grain diameter and solid surface areas (Table 1). This is consistent with the relationships between interfacial areas and grain size and surface areas reported in prior studies (Cary, 1994; Anwar et al, 2000; Costanza and Brusseau, 2000; Cho and Annable, 2005; Peng and Brusseau, 2005; Dobson et al., 2006; Costanza-Robinson et al., 2008; Brusseau et al., 2009; Brusseau et al., 2010).

3.4 Mathematical Modeling

Costanza-Robinson and Henry (2017) conducted a mathematical-modeling study of the potential impact of surfactant-induced flow on air-water interfacial areas measured with the miscible-displacement ITT method. A series of simulations was conducted for hypothetical conditions representative of ITT experiments reported by Costanza-Robinson et al. (2012). The model was not used to simulate actual ITT data sets. Standard and alternative miscible-displacement boundary conditions were employed. Their results showed that the presence of surfactant-induced flow caused deviations of the "measured" interfacial areas, those back-calculated from the simulated breakthrough curves, from the true (input) values. For example, deviations of 14% and 23% were obtained for an initial water saturation of 0.75, depending upon which set of boundary conditions was used.

As discussed above, the interfacial areas measured in the present study with the miscible-displacement ITT method fully match independent measurements produced with methods for which surfactant-induced flow is not relevant by design. This is true for all three media tested, which range from an ideal medium with no surface roughness to a soil that has a very large solid surface area to which microscopic surface roughness contributes greatly. These comparisons demonstrate that the interfacial areas measured by the miscible-displacement ITT method exhibit no deviations from the independent benchmark values. Given that the mathematical modeling results reported by Costanza-Robinson and Henry (2017) show that air-water interfacial areas exhibit deviations when surfactant-induced flow occurs, the absence of deviations in the measured data sets for the present study is another indication that surfactant-induced flow was negligible for the miscible-displacement ITT measurements reported herein.

The results of the mathematical modeling conducted for the present study are presented in Figure 6. Two sets of simulations are presented, one with vacuum applied and one without. The simulation incorporating the vacuum provides a good match to the measured breakthrough curves for SDBS (Figure 6A). In addition, the simulated flux history provides a reasonable match to the measured data, with some of the small perturbations simulated (Figure 6B). These accurate simulations of the measured data are especially noteworthy as the simulations are predictions, wherein values for all input parameters were obtained independently. The ability of a distributed-process model to successfully predict the measured data strongly indicates that the interfacial tracer tests produced robust results consistent with physically-based flow and transport theory and were not impacted by experimental artifacts. To our knowledge, this is the first time that the transport data for an air-water miscible-displacement IT test have been directly simulated with a mathematical model, much less via independent prediction.

Treating the simulated breakthrough curve as a "measured" data set, the air-water interfacial area can be determined based on moment analysis of the data and application of Eq. 1, i.e., employing the standard data analysis used for measured data sets obtained from the ITT method. This application produces interfacial areas of 46.4 and 46.0 cm using moment analysis of the full breakthrough curve and frontal analysis (area above the curve), respectively. These compare well to the measured value of 46.6 cm.

Inspection of Figures 6B and 6C reveals that there was minimal change in effluent flux and column-average water saturation, respectively, during the simulated tracer test with applied vacuum. The modeling results show that employing a vacuum system significantly reduces, and in some cases essentially eliminates, the extent of surfactant-induced flow. This is because adding a vacuum is equivalent to increasing the gravity driving force. Based on Eq. (5), the effective

gravity driving force becomes $-\frac{h_{a,0}}{L} + 1$ times greater (7.8 times in our example simulation) than what it is without a vacuum applied. The perturbation caused by the change of surface tension due to surfactant addition is relatively insignificant compared to the effective gravity driving force, and surfactant-induced flow is therefore greatly reduced. In total, the simulation results demonstrate that there was minimal surfactant-induced flow for the experiment conditions. This is consistent with the results and conclusions reported in the preceding section based on benchmarking analysis of the measured data sets.

Inspection of Figure 6C shows that the water saturation decreases significantly upon introduction of the surfactant solution for the simulation conducted without the vacuum. This denotes an impact of surfactant-induced flow. It is observed that the water saturation recovers to its initial value within \sim 2.5 pore volumes due to the constant-flux boundary at the inlet. This temporal variability of water saturation impacts the flux history and transport of the surfactant. Flux is observed to first increase and then decrease compared to the initial value (Figure 6B). The breakthrough of surfactant is delayed compared to the simulation with vacuum and the measured data (Figure 6A). Another interesting observation is that the simulated breakthrough curve without vacuum applied has a spike wherein the concentration of SDBS is greater than C_0 . The spike is caused by the change in water saturation and the resultant impact on the magnitude of interfacial area. The initial decrease in water saturation upon surfactant introduction creates additional airwater interface, which increases the amount of surfactant adsorbed at the air-water interface. These additional interfaces are eliminated when water saturation increases, thus resulting in transfer of SDBS back to solution.

The mathematical modeling conducted herein demonstrates minimal impact of surfactantinduced flow on the measurement of air-water interfacial areas for the extant conditions of the experiments (vacuum application). This is consistent with the independent-benchmarking analyses reported above. Conversely, significant surfactant-induced flow effects were observed for the simulation that did not employ a vacuum. This latter observation is consistent with the observations of surfactant-induced flow reported by Costanza-Robinson et al. (2012), who used a hanging water-column method for their experiments. It is also consistent with the modeling results of Costanza-Robinson and Henry (2017), who did not incorporate vacuum conditions in their simulations.

Costanza-Robinson and Henry (2017) specifically attempted to address the experiment results reported by Brusseau et al. (2007), for which no surfactant-induced drainage was observed in terms of no change in mean water saturation of the column or in effluent flux. Their simulation results showed significant differences between the calculated and input interfacial areas. Based on this, they concluded that the experiments of Brusseau et al. (2007) were impacted by surfactant-induced flow. Conversely, the results of the independent-benchmarking analyses and the mathematical modeling conducted in the present study clearly demonstrate that surfactant-induced flow did not measurably impact the prior or present experiments. As discussed above, this is due to the application of the vacuum system. Costanza-Robinson and Henry (2017) employed constant-flux conditions for both the upper and lower boundaries to simulate the Brusseau et al. system, which are not representative of the actual experiment conditions. Critically, they did not account for the presence of the vacuum in their simulations. These differences explain the disparity in modeling outcomes obtained.

Kibbey and Chen (2012) also attempted to simulate the interfacial-area measurements reported by Brusseau et al. (2007), using a pore-network model. Their simulated air-water interfacial areas were significantly smaller than the measured values. They attributed this

observation to the impact of some unidentified artifact of the experiment, such as surfactant-induced flow or other factor, presuming that the measured values were in error. However, the measured interfacial areas have been demonstrated to be accurate, as discussed above. The difference in outcomes is related to the simplifications employed in the pore-network modeling, a primary one of which is the assumption that the solid surfaces are smooth (i.e. no surface roughness). It is well established that natural porous media have surface roughness, and several studies have established that such roughness contributes to film-associated interfacial area (e.g., Kim et al., 1999; Or and Tuller, 1999; Schaefer et al., 2000; Brusseau et al., 2007; Jiang et al., 2020). The Vinton soil used in the Brusseau et al. (2007) and present studies in particular has a very large magnitude of roughness. This is manifest in the extreme difference between the nitrogen-BET solid surface area and the geometric smooth-surface solid surface area reported in Table 1, wherein the former is 332-times greater. Not accounting for this roughness and its contribution to interfacial area would lead to artificially smaller simulated interfacial areas.

4. Conclusion

Air-water interfacial areas were measured with the aqueous miscible-displacement ITT method for three porous media—a natural soil, a well-sorted sand, and uniform glass beads. The results of replicate tests showed that the standard IPTT method employing the vacuum-chamber system provided excellent reproducibility and precision in the ability to obtain a target water saturation and in the measurement of interfacial area. The interfacial areas obtained for the soil are larger than the values for the sand and the glass beads. This is consistent with the relationship between grain size, pore size, and surface area, and their impact on interfacial area.

No significant changes in water saturation or flux were observed for the tests conducted with the vacuum-chamber system. Independent predictions produced with a flow and transport model provided very good matches to the measured SDBS transport and solution flux, and revealed that surfactant-induced flow was negligible under the extant conditions. The most definitive way to effectively evaluate the accuracy of a particular measurement method is to compare measured values produced with the method to independent benchmarks. Air-water interfacial areas measured with the miscible-displacement ITT method were compared to values measured by four different methods, each of which are by design exempt from surfactant-induced flow. The air-water interfacial areas measured with the standard ITT method were completely consistent with the values measured by the alternative methods.

The results reported herein unequivocally demonstrate that the air-water interfacial areas measured by the miscible-displacement ITT method in this study and the prior study of Brusseau et al. (2007) are accurate, and were not measurably impacted by surfactant-induced flow. This outcome encompasses results for three porous media with great differences in surface roughness and for a relatively wide range of water saturations. Clearly, surfactant-induced flow can affect miscible-displacement IT tests under certain conditions, as demonstrated in prior studies. Hence, it is critical to assess its potential occurrence and impact for each application. However, it is important to recognize that surfactant-induced flow and its impacts are not endemic to all applications of the method. Costanza-Robinson and Henry (2017) and Kibbey and Chen (2012) both suggested that air-water interfacial areas determined with the miscible-displacement ITT method have significant uncertainty in all cases, questioning the utility of the method in general. The results of the present study demonstrate that the method does produce accurate measurements, as long as it is implemented in a manner that minimizes or eliminates surfactant-induced flow. In

the present case, this was accomplished by employing a vacuum system. It can also be accomplished for example by employing low tracer-input concentrations (Brusseau et al., 2020b) or dual-surfactant solutions (Brusseau et al., 2015). This study should help to resolve potential misconceptions and concerns about the general efficacy of the miscible-displacement ITT method.

508

509

510

511

512

513

504

505

506

507

Acknowledgments

This research was funded by the NIEHS Superfund Research Program (Grant #P42 E504940) and the National Science Foundation (2023351). We thank the reviewers for their constructive comments. All measured interfacial area data discussed in this work are presented in the accompanying figures.

514

515

References

- Anderson, R.H., Adamson, D.T., Stroo, H.F., 2019. Partitioning of poly-and perfluoroalkyl
- substances from soil to groundwater within aqueous film-forming foam source zones. *J. Contam.*
- 518 *Hydrol.*, 220, 59-65.

519

- Anwar, A., M. Bettahar, and U.J. Matsubayashi (2000). A method for determining air-water
- 521 interfacial area in variably saturated porous media, *J. Contam. Hydrol.*, 43, 129–146.

522

- Anwar, A. (2001). Experimental determination of air—water interfacial area in unsaturated sand
- medium. New Approaches Characterizing Groundwater Flow. In: Proceedings. of XXXI IAH
- 525 Congress, Munich, Germany, September 10–14, Vol. 2, pp. 821–825.

526

- 527 Araujo, J.B., and Brusseau, M.L. (2020). Assessing XMT measurement variability of air -
- water interfacial areas in natural porous media. Water Resour Res, 56,
- 529 doi:10.1029/2019WR025470.

- Araujo, J.B., J. Mainhagu, and M.L. Brusseau (2015). Measuring air-water interfacial area for
- soils using the mass balance surfactant-tracer method. *Chemosphere* 134, 199–202.

- Brusseau, M.L. (2018). Assessing the potential contributions of additional retention processes to
- PFAS retardation in the subsurface. Sci. Total Environ., 613-614, 176-185.

536

- Brusseau, M. L. (2020). Simulating PFAS transport influenced by rate-limited multi-process
- retention. Water Research, 168, 115179.

539

- Brusseau, M.L., J. Popovicova, and J.A.K. Silva (1997). Characterizing gas-water interfacial and
- bulk-water partitioning for gas-phase transport of organic contaminants in unsaturated porous
- 542 media, Environ. Sci. Technol., 31, 1645–1649.

543

- Brusseau, M.L., S. Peng, G. Schnaar, and A. Murao (2007). Measuring air-water interfacial areas
- with x-ray microtomography and interfacial partitioning tracer tests. *Environ. Sci. Technol.*, 41(6),
- 546 1956-1961.

547

- Brusseau, M.L., M. Narter, S. Schnaar, and J. Marble (2009). Measurement and estimation of
- organic liquid/water interfacial areas for several natural porous media, Environ. Sci. Technol.,
- 550 *43*(10), 3619–3625.

551

- Brusseau, M.L., M. Narter, and H. Janousek (2010). Interfacial partitioning tracer test
- 553 measurements of organic-liquid/water interfacial areas: application to soils and the influence of
- surface roughness, Environ. Sci. Technol., 44(19), 7596-7600.

555

- Brusseau, M.L., A. El Ouni, J.B. Araujo, and H. Zhong (2015). Novel methods for measuring
- air-water interfacial area in unsaturated porous media, *Chemosphere*, 127, 208–213.

- Brusseau, M.L., Yan, N., Van Glubt, S., Wang, Y., Chen, W., Lyu, Y., Dungan, B., Carroll, K.C.,
- Holguin, F.O. (2019). Comprehensive retention model for PFAS transport in subsurface systems.
- 561 *Water Res.* 148, 41-50.

- Brusseau, M.L., R.H. Anderson, and B, Guo (2020a). PFAS concentrations in soils: background
- levels versus contaminated sites. Sci. Total Environ., 740, article 140017.

565

- Brusseau, M.L., Y. Lyu, N. Yan, and G. Guo (2020b). Low-concentration tracer tests to measure
- air-water interfacial area in porous media. *Chemosphere*, 25, doi:
- 568 10.1016/j.chemosphere.2020.126305.

569

- Buffham, B.A. (1973). Model-independent aspect of tracer chromatography theory. *Proc. R.*
- 571 *Soc. Lond. A.*, 333, 89–98.

572

- 573 Cary, J.W. (1994). Estimating the surface area of fluid phase interfaces in porous media. J.
- 574 *Contam. Hydrol.*, 15, 243–248.

575

- 576 Cho, J., and M.D. Annable (2005). Characterization of pore scale NAPL morphology in
- 577 homogeneous sands as a function of grain size and NAPL dissolution, *Chemosphere*, 61, 899–908.

578

- 579 Costanza- Robinson, M.S., and M.L. Brusseau (2000). Contaminant vapor adsorption at the gas-
- water interface in soils, *Environ. Sci. Technol.*, 34(1), 1-11.

581

- Costanza-Robinson, M.S., and M.L. Brusseau (2002). Air-water interfacial areas in unsaturated
- 583 soils: Evaluation of interfacial domains, Water Resour. Res., 38(10), 1195, doi:
- 584 10.1029/2001WR000738.

- 586 Costanza-Robinson, M.S. and E.J. Henry (2017). Surfactant-induced flow compromises
- determination of air-water interfacial areas by surfactant miscible-displacement. Chemosphere
- 588 171, 275-283.

- Costanza-Robinson, M.S., K.H. Harrold, and R.M. Lieb-Lappen (2008). X-ray microtomography
- determination of air-water interfacial area-water saturation relationships in sandy porous media.
- *Environ. Sci. Technol*, 42(8), 2949–2956, doi: 0.1021/es072080d.

593

- Costanza-Robinson, M.S., Z. Zheng, E.J. Henry, B. D. Estabrook, and M.H. Littlefield (2012).
- 595 Implications of surfactant-induced flow for miscible-displacement estimation of air-water
- interfacial areas in unsaturated porous media, *Environ. Sci. Technol.*, 46(20), 11206-11212.

597

- 598 Dong, S., B. Gao, Y. Sun, Z. Shi, H. Xu, J. Wu, and J. Wu (2016). Transport of sulfacetamide and
- 599 levofloxacin in granular porous media under various conditions: Experimental observations and
- model simulations. Sci. Total Environ., 573, 1630-1637.

601

- 602 Glueckauf, E. (1955). Theory of chromatography. Part 9. The "theoretical plate" concept in
- 603 column separations." J. Chem. Soc. Faraday Trans., 51, 34–44.

604

- 605 Guo, B., J. Zeng, and M.L. Brusseau, (2020). A mathematical model for the release, transport,
- and retention of per- and polyfluoroalkyl substances (PFAS) in the vadose zone. *Water Resour*.
- 607 Res., 57, doi: 10.1029/2019WR026667.

608

- Jiang, H., B. Guo, and M.L. Brusseau (2020). Pore-scale modeling of fluid-fluid interfacial area
- in variably saturated porous media containing microscale surface roughness. Water Resour. Res.,
- 611 *56*, doi:10.1029/2019WR025876.

612

- Karkare, M.V., T. Fort (1996). Determination of the air-water interfacial area in wet
- "unsaturated" porous media. Langmuir, 12, 2041–4044.

615

- Kim, H., P.S.C. Rao, and M.D. Annable (1997). Determination of effective air-water interfacial
- area in partially saturated porous media using surfactant adsorption. Water Resour. Res., 33(12),
- 618 2705-2711.

- 620 Kim, H. M.D. Annable, and P.S.C. Rao (1998). Influence of air-water interfacial adsorption and
- gas-phase partitioning on the transport of organic chemicals in unsaturated porous media.
- 622 Environ. Sci. Technol., 32, 1253-1259.

- Kim, H., P.S.C. Rao, and M.D. Annable (1999). Gaseous tracer technique for estimating air-water
- interfacial areas and interface mobility, Soil Sci. Soc. Am. J., 63, 1554–1560.

626

- Kucera, E. (1965). Contribution to the theory of chromatography linear non-equilibrium elution
- 628 chromatography. J. Chromatogr., 19, 237–248.

629

- Kumahor, S.K., P. Hron, G. Metreveli, G. E. Schaumann, and H-J. Vogel (2015). Transport of
- citrate-coated silver nanoparticles in unsaturated sand. Sci. Total Environ., 535, 113-121.

632

- Lyu, Y., Brusseau, M.L., Chen, W., Yan, N., Fu, X., Lin, X., 2018. Adsorption of PFOA at
- the air-water interface during transport in unsaturated porous media. *Environ. Sci. Technol.* 52,
- 635 7745-7753.

636

- 637 Lyu, Y., and M. L., Brusseau (2020). The influence of solution chemistry on air-water interfacial
- adsorption and transport of PFOA in unsaturated porous media. Sci. Total Environ., 713, 136744.

639

- Makselon, J., D. Zhou, I. Engelhardt, D. Jacques, and E. Klumpp (2017). Experimental and
- numerical investigations of silver nanoparticle transport under variable flow and ionic strength in
- 642 soil. Environ. Sci. Technol., 51,2096–2104.

643

- Mualem, Y. (1976). A new model for predicting the hydraulic conductivity of unsaturated porous
- 645 media. Water Resour. Res., 12(3), 513-522.

646

- Narter, M., and M. L. Brusseau (2010). Comparison of interfacial partitioning tracer test and high-
- resolution microtomography measurements of fluid-fluid interfacial areas for an ideal porous
- 649 medium. Water Resour. Res., 46, W08602, doi: 10.1029/2009WR008375.

Or, D., and M. Tuller (1999). Liquid retention and interfacial area in variably saturated porous media: Upscaling from single-pore to sample-scale model, Water Resour. Res., 35, 3591–3605. Peng, S., and M.L. Brusseau (2005). The impact of soil texture on air-water interfacial areas in unsaturated sandy porous media, Water Resour. Res., 41, W03021, doi: 0.1029/2004WR003233. Saripalli, K. P., H. Kim., P. S. C. Rao, M. D. Annable (1997). Measurement of specific fluid-fluid interfacial areas of immiscible fluids in porous media, Environ. Sci. Technol., 31(3), 932-936. Schaefer, C.E., D.A. DiCarlo, and M.J. Blunt (2000). Experimental measurement of air-water interfacial area during gravity drainage and secondary imbibition in porous media, Water Resour. Res., 36, 885–890. Valocchi, A.J. (1985). Validity of the local equilibrium assumption for modeling sorbing solute transport through homogeneous soil. Water Resour. Res., 21, 808-820. Van Genuchten, M. T. (1980). A closed-form equation for predicting the hydraulic conductivity of unsaturated soils 1. Soil Sci. Soc. Amer. J., 44(5), 892-898.

Table 1. Relevant physical properties of the porous media used in the experiments

Medium	Median diameter d ₅₀ (mm)	Uniformity coefficient U ^a	Geometric SSSA ^b (cm ⁻¹)	N ₂ /BET SSSA ^c (cm ⁻¹)
Vinton	0.23	2.4	160	53100
Sand	0.35	1.1	115	1800
Glass Beads	1.16	1.0	31	30

 $^{^{}a}U = (d_{60}/d_{10}).$

Table 2. Analysis of experiment replication [Vinton soil data]

Source	Method	Status	S_{w}	A _{ia} (cm ⁻¹)
This study	Standard	Drainage	0.810	73.9
This study	Standard	Drainage	0.820	69.0
This study	Standard	Drainage	0.817	62.1
This study	Standarda	Drainage	0.801	63.6
This study	Standard	Imbibition	0.805	60.5
Brusseau et al.	Standard	Imbibition	0.810	55.5
2007				
Brusseau et al.	Standard	Imbibition	0.818	78.6
2007				
Mean			0.81	66.2
95% CI ^b			0.005	6.0
COV (%)°			0.6	9
Brusseau et al.	Dual Surfactant	Drainage	0.81	61.0
2015				
Brusseau et al.	Residual Air	Sec. Imbibition	0.81	61.3
2015				

 $[^]aA$ vacuum system without the enclosed chamber was used for this experiment; the mean S_w of the column decreased temporarily by ${\sim}7\%$ during the experiment.

^b Geometric smooth-surface specific solid surface area (SSSA): 6(1-n)/d, where n is the porosity and d is the median grain diameter.

^c Specific solid surface area measured by the N₂/BET method.

^b95% confidence interval

^ccoefficient of variation based on the 95% CI

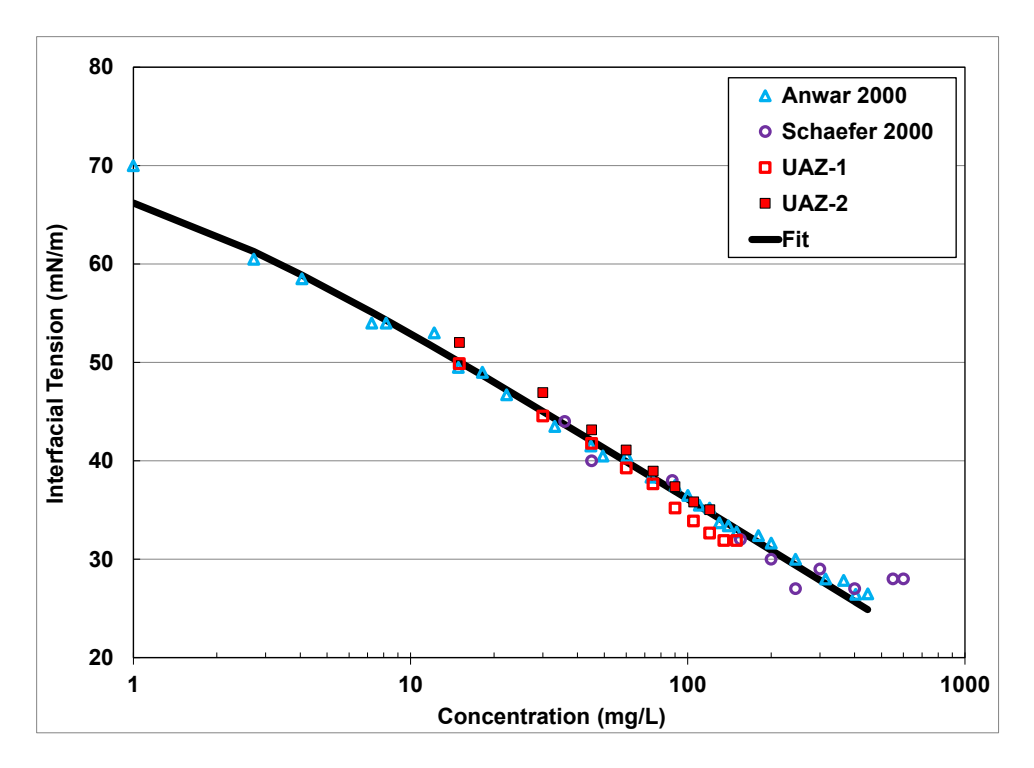
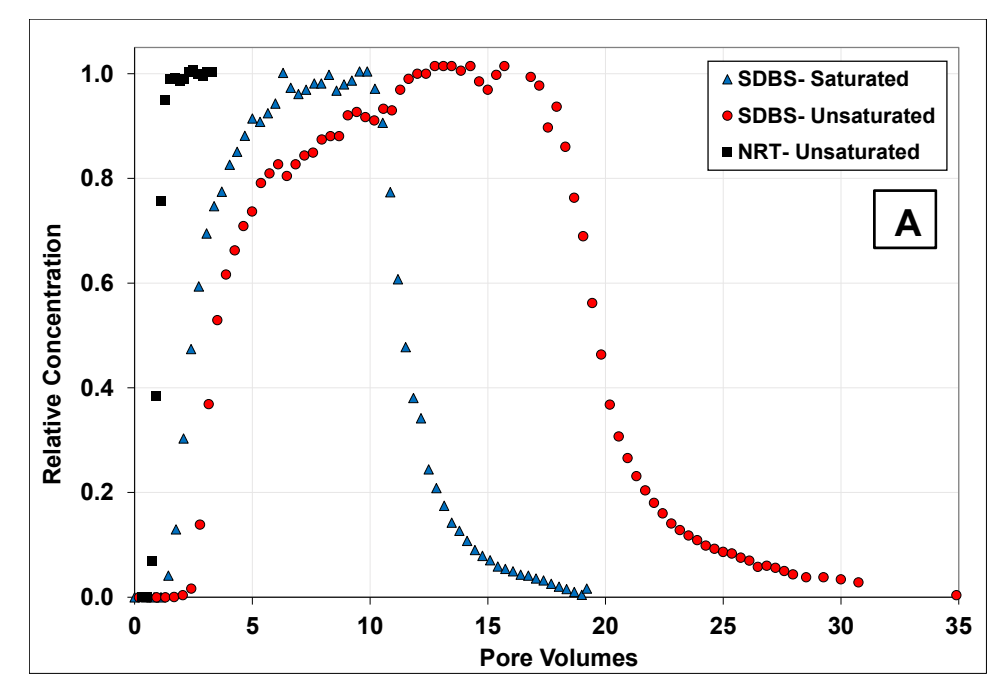


Figure 1. Surface tension data sets for SDBS measured in 0.01 M NaCl solution. UAZ-1 and UAZ-2 denote measurements made for the present study, at different times. The fit is produced with application of the Szyszkowski equation.



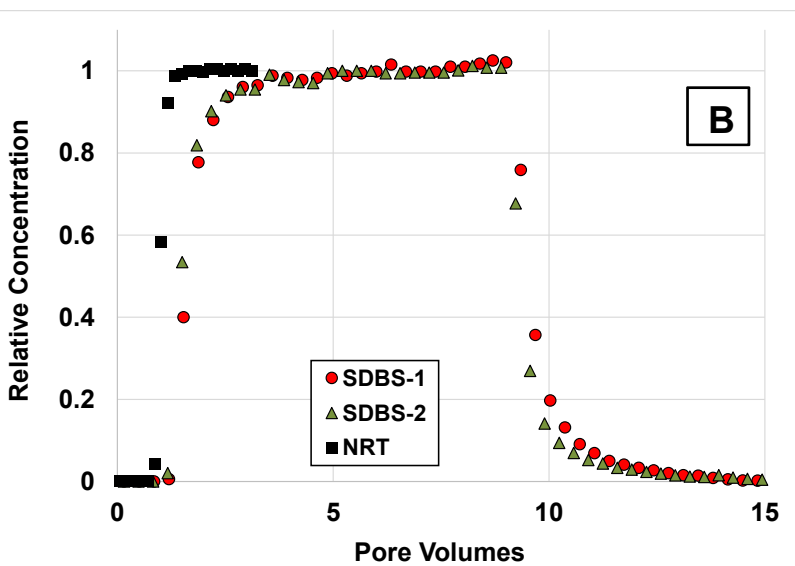


Figure 2. Example breakthrough curves for SDBS transport in (A) Vinton soil (for saturated and unsaturated conditions) and (B) sand (for unsaturated conditions). NRT = non-reactive tracer

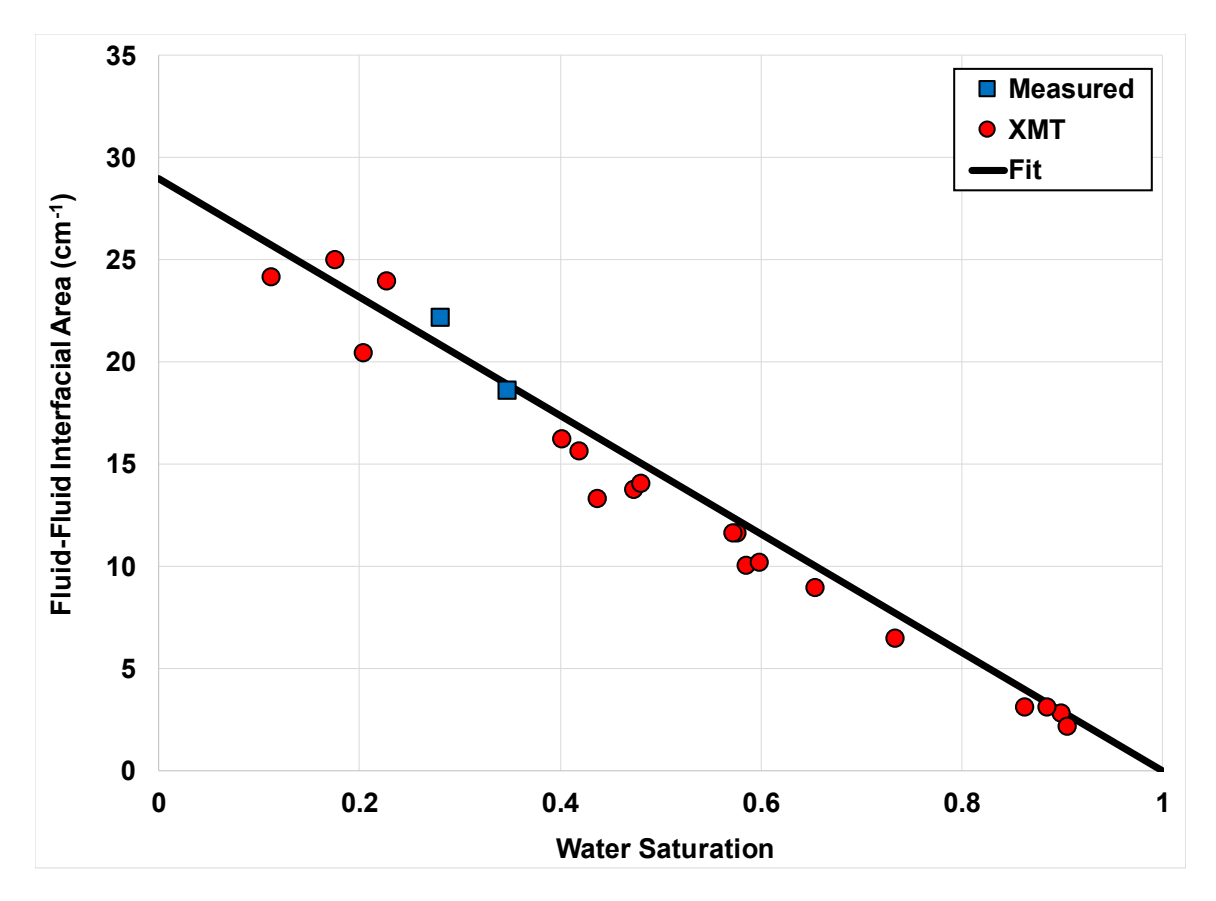


Figure 3. Air-water interfacial areas measured with the miscible-displacement interfacial tracer method and by x-ray microtomography (XMT) for glass beads. XMT data reported by Araujo and Brusseau (2020). The line represents the best fit to the XMT data.

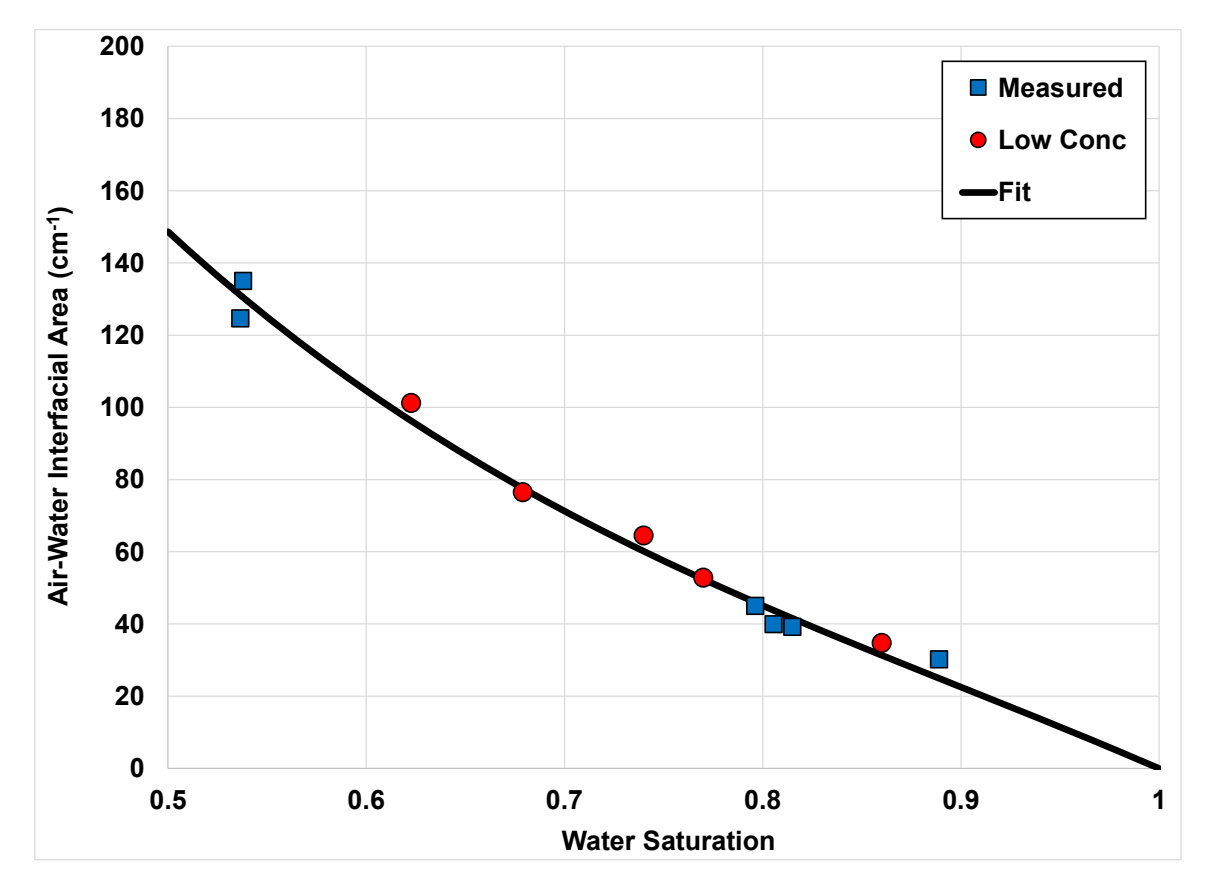


Figure 4. Air-water interfacial areas measured with the miscible-displacement interfacial tracer method for sand. The "Low Conc" data were measured using tracer-input concentrations ≤ 1 mg/L for which there was no measurable surfactant-induced flow; data reported by Brusseau et al. (2020). The curve represents the best fit to the ensemble data set.



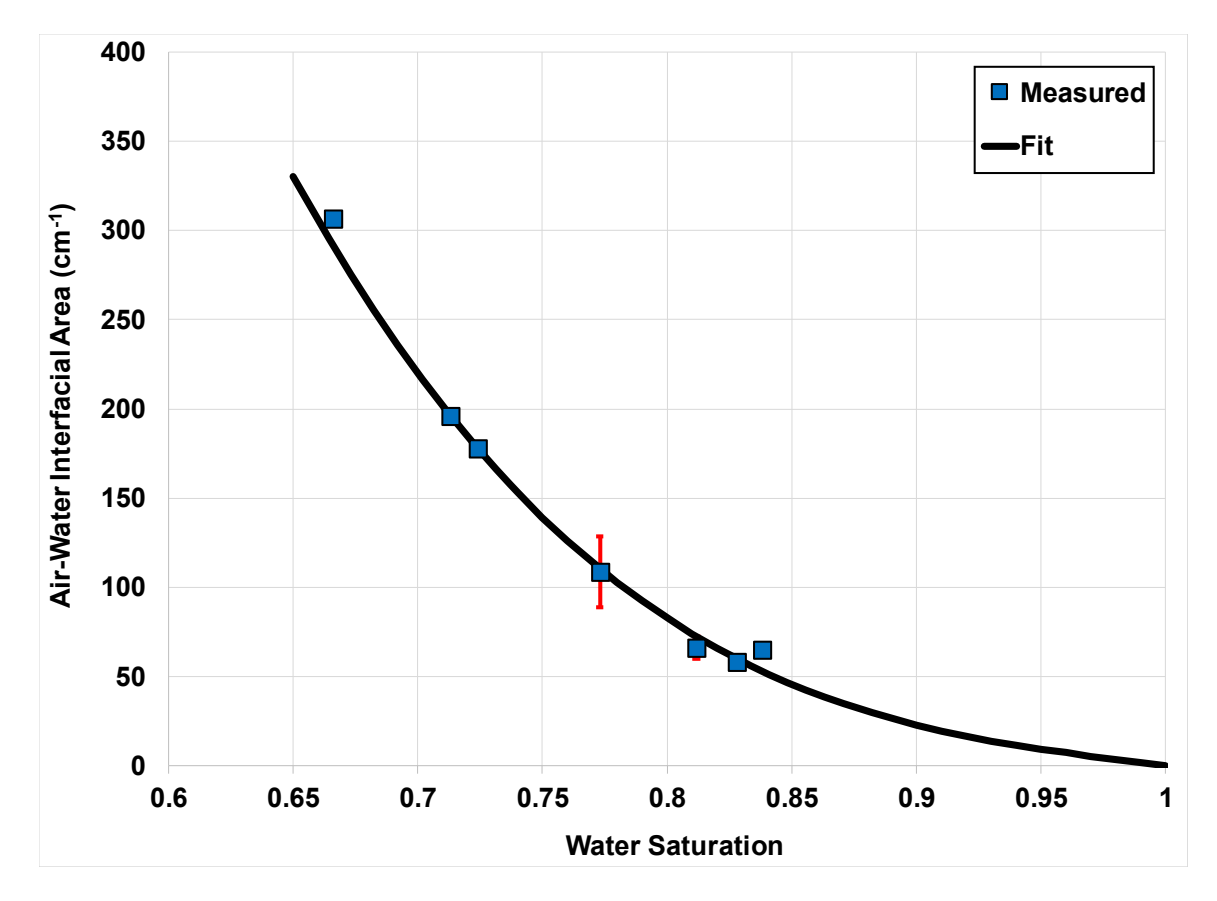
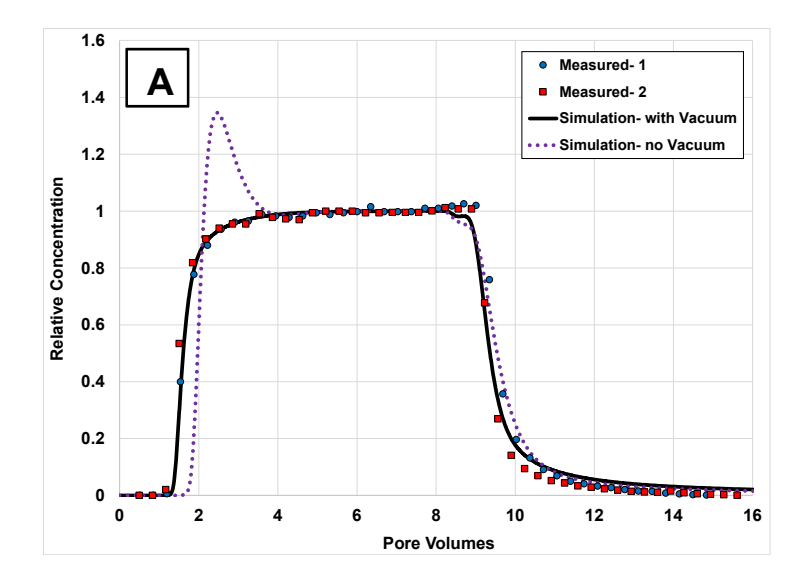
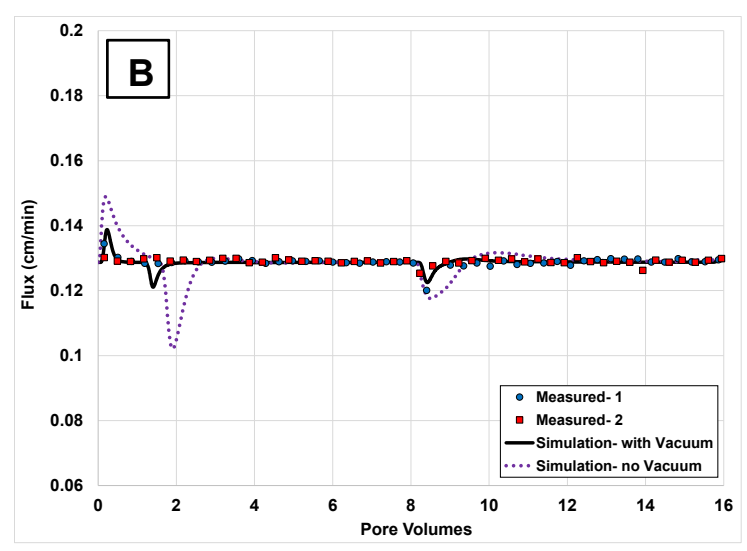


Figure 5. Air-water interfacial areas measured with the miscible-displacement interfacial tracer method for Vinton soil. Red vertical bars are the 95% confidence intervals. Some of these data were reported previously in Brusseau et al. (2007). The curve represents the best fit to the data set.





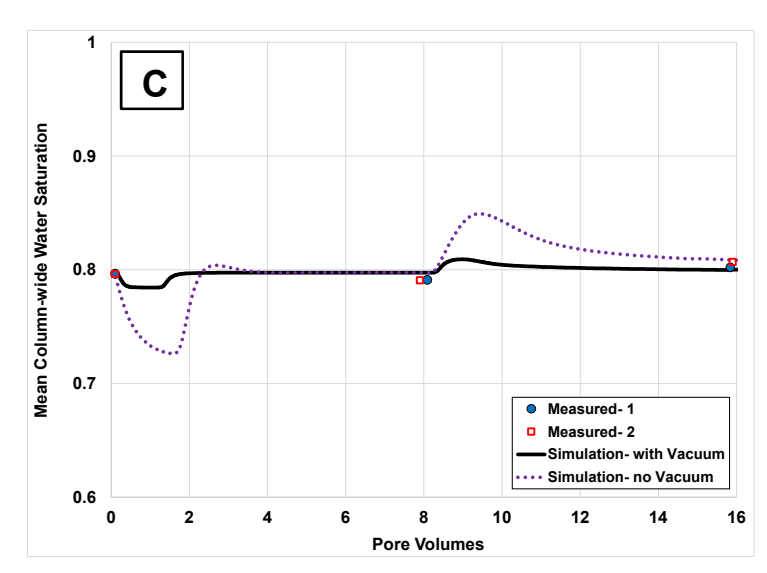


Figure 6. Simulated and measured results for a representative miscible-displacement interfacial tracer test. (A) breakthrough curves for SDBS transport in the sand. (B) effluent solution flux. (C) column-average water saturation.